GBE

Stability of Mitochondrial Membrane Proteins in Terrestrial Vertebrates Predicts Aerobic Capacity and Longevity

Yasuhiro Kitazoe*[,1], Hirohisa Kishino[2], Masami Hasegawa[3,4], Atsushi Matsui[5], Nick Lane[6], and Masashi Tanaka[7]

[1]Center of Medical Information Science, Kochi Medical School, Nankoku, Kochi, Japan

[2]Graduate School of Agricultural and Life Sciences, University of Tokyo, Yayoi, Bunkyo, Tokyo, Japan

[3]School of Life Sciences, Fudan University, Shanghai, China

[4]Institute of Statistical Mathematics, Tokyo, Japan

[5]Department of Cellular and Molecular Biology, Primate Research Institute, Kyoto University, Inuyama-city, Aichi, Japan

[6]Department of Genetics, Evolution and Environment, University College London, United Kingdom

[7]Department of Genomics for Longevity and Health, Tokyo Metropolitan Institute of Gerontology, Japan

*Corresponding author: E-mail: kitazoeyasuhiro@yahoo.co.jp.

Accepted: 23 July 2011

Abstract

The cellular energy produced by mitochondria is a fundamental currency of life. However, the extent to which mitochondrial (mt) performance (power and endurance) is adapted to habitats and life strategies of vertebrates is not well understood. A global analysis of mt genomes revealed that hydrophobicity (HYD) of mt membrane proteins (MMPs) is much lower in terrestrial vertebrates than in fishes and shows a strong negative correlation with serine/threonine composition (STC). Here, we present evidence that this systematic feature of MMPs was crucial for the evolution of large terrestrial vertebrates with high aerobic capacity. An Arrhenius-type equation gave positive correlations between STC and maximum life span (MLS) in terrestrial vertebrates (with a few exceptions relating to the lifestyle of small animals with a high resting metabolic rate [RMR]) and negative correlations in secondary marine vertebrates, such as cetaceans and alligators (which returned from land to water, utilizing buoyancy with increased body size). In particular, marked STC increases in primates (especially hominoids) among placentals were associated with very high MLS values. We connected these STC increases in MMPs with greater stability of respiratory complexes by estimating the degradation of the Arrhenius plot given by accelerating mtRMR up to mt maximum metabolic rate. Both mtRMR and HYD in terrestrial vertebrates decreased with increasing body mass. Decreases in mtRMR raise MMP stability when high mobility is not required, whereas decreased HYD may weaken this stability under the hydrophobic environment of lipid bilayer. High maximal metabolic rates (5–10 RMR), which we postulate require high MMP mobility, presumably render MMPs more unstable. A marked rise in STC may therefore be essential to stabilize MMPs, perhaps as dynamic supercomplexes, via hydrogen bonds associated with serine/threonine motifs.

Key words: vertebrate evolution, mitochondrial membrane protein stability, hydrophobicity, serine/threonine composition, aerobic capacity, longevity.

Introduction

One of the most dramatic macroevolutionary events in vertebrate history was the water-to-land transition. Extant amphibians highlight the adaptive challenges facing this transition. Terrestrial vertebrates needed large increases in cellular energy budget and developed a powerful lung-based respiratory and cardiovascular system. However, the mechanism by which their metabolic rates vary so substantially remains poorly understood at both the physiological and the mitochondrial (mt) levels (Lane 2006; Pontzera et al. 2010). Each group of vertebrates has its own characteristic history of evolutionary adaptation to new habitats and life

strategies. If this history is preserved in mt genomes, a comparative study across various vertebrate groups may detect new aspects of mt functions and answer the long-standing question of whether large variations in mtDNA sequences are due to adaptive evolution of amino acid sequences (Grossman et al. 2001; Goldberg et al. 2003; Kitazoe et al. 2008; Min and Hickey 2008; Moosmann and Behl 2008) or nucleotide mutation pressure (Reyes et al. 1998; Schmitz et al. 2002; Gibson et al. 2005; Jobson et al. 2010).

Previous studies have attempted to connect the evolutionary rate of mtDNA to macroscopic traits such as resting metabolic rate (RMR), body weight (*W*), and maximum life span (MLS) of vertebrates. The evolutionary rate is inversely related to *W* (Bromham et al. 1996; Gillooly et al. 2007) and quite variable across species in short-lived mammals but constrained to low values in long-lived mammals (Welch et al. 2008). Long-lived mammals and birds may have increased their MLS in part by evolving macromolecular components that are more resistant to oxidative damage (Pamplona and Barja 2007; Min and Hickey 2008). The evolution of mtDNA shows a large variation in substitution rates between various lineages (Spradling et al. 2001; Kitazoe et al. 2008; Nabholz et al. 2009). For example, mtDNA sequences in higher primates evolved twice as fast as other placental mammals (Kitazoe et al. 2008) and birds evolved at a quarter the speed of placentals (Nabholz et al. 2009). From this standpoint, Galtier et al. (2000) recently argued that a direct mechanical effect of RMR on mtDNA evolutionary rate is unlikely and that natural selection could act to reduce the mtDNA mutation rate in long-lived species.

Other studies have focused on a compositional analysis of the mt constituents. A correlation between cysteine composition and MLS has been proposed as cysteine depletion may render mt proteins more resistant to oxidative attack and loss of mt membrane protein (MMP) mobility through protein cross-linking (Moosmann and Behl 2008). Mammals and birds show a strong negative correlation between MLS and the proportion of $n-3$ polyunsaturated fatty acids in lipids, the side chains of which are sensitive to peroxidation (Pamplona et al. 2002; Hulbert et al. 2007). Mammals also show significant correlations between GC content and MLS (Lehmann et al. 2008). A detailed tree analysis along the primate lineage demonstrated that a predominant T→C flow at second codon sites in the higher primate lineage induced a marked Thr increase, which is positively correlated with MLS (Kitazoe et al. 2008). These compositional analyses strongly suggest adaptation of the mt protein constituents.

In the present study, our global analysis of vertebrates suggests that the HYD decreases and serine/threonine composition (STC) increases in MMPs might have played a fundamental role in increasing the aerobic capacity of terrestrial vertebrates after the water-to-land transition. Higher STC values in terrestrial vertebrates were closely associated with longer life spans. An extreme enhancement of this trend appeared in the primate lineage. Conversely, secondary marine vertebrates such as cetaceans and alligators, which utilize buoyancy without the constraints of gravity, contrasted sharply with the trend in terrestrial vertebrates. We show that rodents and insectivores display no STC–MLS correlation because STC content saturates at high RMR but instead show a strong negative correlation between MLS and cysteine composition sensitive to oxidative damage and free radical leak (Moosmann and Behl 2008). To explain the STC–MLS correlation, we tested the stability of MMPs to the marked HYD decrease and STC increase in primates by using the Arrhenius plot analysis (Lachman and DeLuca 1976; Ertel and Carstensen 1990; Carstensen 2000). By accelerating the mt metabolic rate from the resting rate to the maximum rate in the Arrhenius equation, we predict that stabilizing MMPs by the additional STC increases results in further longevity prolongation of primates (hominoids). Finally, we demonstrate that a short-range hydrogen bonding potential to stabilize MMPs can be effectively transformed into a long-range dynamic anchoring of MMPs, which we postulate may assist the formation of respirasome supercomplexes at high metabolic rates (Acín-Pérez et al. 2008; Genova et al. 2008; Lenaz and Genova 2009).

Materials and Methods

Data Retrieval

MLS, RMR, and *W* data were obtained from the AnAge database (http://genomics.senescence.info/species/; de Magalhaes and Costa 2009; Secor 2003), the Max Planck Institute database (http://www.demogr.mpg.de/longevityrecords/; Garey and Judge 2002), and Moosmann and Behl (2008). Seven hundred and seventy-one complete mtDNA sequences of vertebrates were obtained from the NCBI genome database (http://www.ncbi.nlm.nih.gov/genomes/). The 228 species with the same scientific names in the AnAge and NCBI genome databases were collected for the present longevity analysis. Although *W* data are normally available for these species, RMR data are frequently lacking. Fortunately, because the correlations between these two values are excellent (the correlation coefficient for placentals is 0.983 and that for birds is 0.999), approximate RMR values were obtained by using the regression line as a function of *W* if the data are not available.

Maximum Life Span Analysis Using an Arrhenius-Type Equation

This paper presents a procedure of how to relate mt functions to the MLS of an organism. The mitochondrion is a semiautonomous organelle with its own genome and life span (L_{mt}). The life span L_{mt} is confounded by the flux rate through mt fission and fusion and mitophagy quality control (Twig and Shirihai 2011). We assume that greater MMP

stability delays the turnover of MMP complexes and so prolongs the abstract quantity L_{mt}. Therefore, we primarily have to formulate a relationship between mt functions and this life span. Electron transport and oxidative phosphorylation are critical activities of the MMP complexes. Electrons are transported along the mt respiratory chain, via quantum tunneling between redox centres, to generate a proton gradient. Although the exact distance between redox centers is critical to electron flux (Moser et al. 2006), the overall kinetics of oxidative phosphorylation are consistent with the dynamic assembly and disassembly of respirasome supercomplexes (Acín-Pérez et al. 2008; Genova et al. 2008); hence, both the stability and the mobility of MMPs are required for respiratory function, especially at high maximal metabolic rate. Electrochemical energy of electron transfer is utilized for ATP production and thermogenesis, but some of the leaked electrons react with oxygen to generate reactive oxygen species, which are mutagenic signaling molecules. In this way, the MMP complexes act like a battery in a thermal equilibrium of temperature T_{mt}. Then, L_{mt} is given by Arrhenius equation for chemical reactions, $L_{mt} = C_0 \exp\{C_1/(kT_{mt})\}$ with constants C_0, C_1 and Boltzmann constant k (Arrhenius equation is generally applied to estimate the shelf life and stability of drugs: Lachman and DeLuca 1976; Ertel and Carstensen 1990; Carstensen 2000). As an extension of this equation, we here apply a temperature–humidity model, $L_{el} = C_0 \exp(C_1/T_{el} + C_2/H_{el})$, to test electronic devices at different temperature (T_{el}) and humidity (H_{el}) conditions (Accelerated Life Testing Analysis Theory & Principles) because we may replace the device property H_{el} by STC and HYD of MMPs assuming that L_{mt} and kT_{mt} are proportional to MLS of an organism and mtRMR in the resting metabolic state, respectively. Then, we obtain

$$Y = \ln(\mathrm{MLS}) = A_1/\mathrm{mtRMR} + A_2/\mathrm{STC} + A_3/\mathrm{HYD} + A_0 = A_1X_1 + A_2X_2 + A_3X_3 + A_0, \quad (1)$$

with constants A_n ($n = 0$–3).

When the total number of cells in an organism is proportional to W, we can write $\mathrm{mtRMR} = \mathrm{RMR}/W^q$. Here, a constant q less than 1 takes into account the property that the mt density within cells may fall with increasing W (Porter and Brand 1995; Porter 2001) and is determined so as to maximize the correlation R_{1Y} between X_1 and Y. Equation (1) is useful when the life span (L_{cell}) of cells is sufficiently long compared with L_{mt} (stem cells fulfill this condition). Using the variables X_1, X_2, and X_3 in place of mtRMR, STC, and HYD, respectively, we can follow a standard multiple regression analysis. The theoretical value Y to estimate MLS is sensitive to small mtRMR values because it is expressed in terms of 1/mtRMR. We here note that the expression (1) is comprehensive and can include any other variables X_n ($n > 3$), if necessary. The importance of this inclusion will be automatically evaluated by the multiple regression analysis.

Selection of Hydrophobic Domains in MMPs

To select hydrophobic domains in MMPs, we applied the primary structure analysis (ExPASy Proteomics Server; http://www.expasy.ch/; Gasteiger et al. 2005), using a standard model for the hydrophobic score (S) (Cowan and Whittaker 1990). We calculated the moving average, S_{av}, of local hydrophobic scores S (with a window of five amino acid sites) around each amino acid site. HYD of each vertebrate is defined as the average value of S_{av} values, which are restricted to a hydrophobic domain of MMPs. The primary structure analysis has an accuracy of 80% to discriminate between the helix domain and the nonhelix domain of MMPs. HYD values depend on a model of a hydrophobic score being applied. However, our approach was sufficient to propose quite a fundamental theory as to how MMP functions responded to the transition of vertebrates from water to land and in different groups on land.

Results

Global Relationship between STC and HYD in MMPs of Vertebrates

The water-to-land transition of vertebrates was one of the most dramatic events in vertebrate evolutionary history. We therefore began our analysis by extracting amino acid compositions in MMPs, which most changed in tandem with this development. For this purpose, simply dividing the 771 vertebrate mt sequences (obtained from the NCBI genome database) into two groups of fishes (382) and nonfishes (389) ("Materials and Methods"), we made the t-test for difference of means of amino acid composition values between these two groups. As a result, we found that HYD provides a very good separation ($t = 16.32$ and $P < 10^{-21}$) of HYD distribution into the two groups without any constraints on MMPs. Selecting seven proteins (ND3, ND4, CO1, CO2, ATP6, ATP8, and CYTB) within MMPs furthermore improved the separation rate with $t = 42.52$ and $P < 10^{-80}$ (fig. 1A), although the original separation without this constraint is in itself excellent.

We next selected amino acids that are negatively correlated with HYD. Here, HYD stands for the average value of S_{av} values in a hydrophobic domain, which includes the amino acid sites (with $S_{av} > c$, and c is a constant) of MMPs to be specified in an animal group, and S_{av} denotes the moving average of local hydrophobic scores S around an amino acid site (Materials and Methods. Table 1 shows that the correlations of threonine and serine with HYD are much better than other amino acids as higher hydrophobic domains are selected by the S_{av} value of each amino acid site. This trend became clearer in the helix domain roughly estimated by the primary structure analysis, especially when the estimated helix region with very low S_{av} values ($S_{av} < 0.1$) is further excluded and the nonhelix region with very high S_{av} values ($S_{av} > 0.7$) is included (the red letters

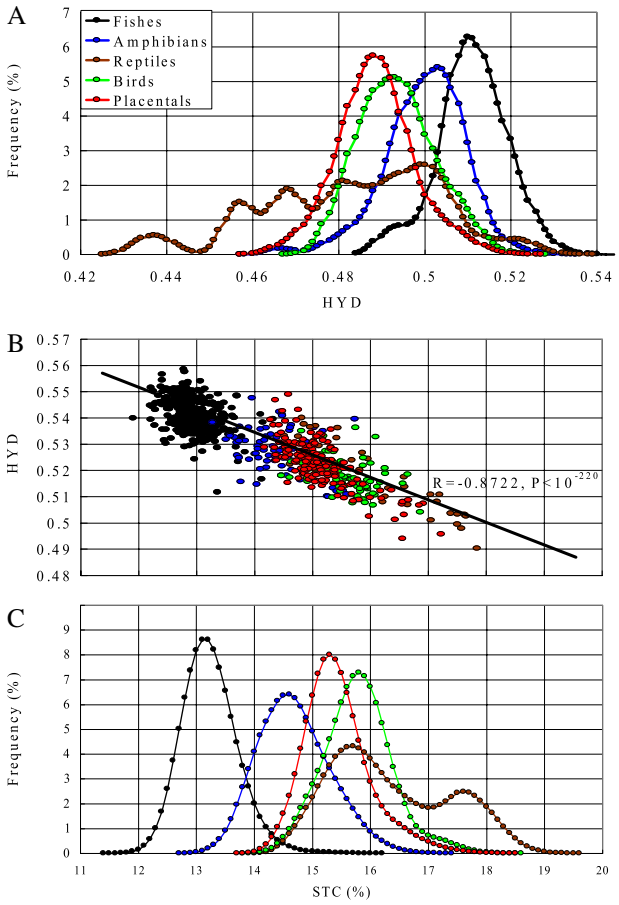

Fig. 1.—(*A*) Frequency distribution of HYD over vertebrates. (*B*) Correlation between STC and HYD. (*C*) Frequency distribution of STC. The correlation became very strong in a hydrophobic domain of $S_{av} < 0.05$ ($R = -0.8722$ and $P < 10^{-220}$). Here, S_{av} is the moving average of local hydrophobic scores S around each amino acid site (Materials and Methods).

Table 1

Threonine and Serine Strongly Correlated with HYD in Hydrophobic Domains of MMPs

	Inclusive	$S_{av} > 0$	$S_{av} > 0.2$	Helix	Helix cut
1) Ala	0.655	0.658	0.356	0.377	0.389 ($P < 10^{-28}$)
2) Arg	0.606	0.575	0.380	0.254	0.252 ($P < 10^{-11}$)
3) Asn	−0.639	−0.675	−0.339	−0.490	−0.467 ($P < 10^{-42}$)
4) Asp	0.383	0.536	0.474	0.021	0.024 ($P < 0.6$)
5) Cys	0.020	0.068	−0.092	0.036	0.019 ($P < 0.5$)
6) Gln	−0.090	−0.119	−0.137	−0.540	−0.454 ($P < 10^{-39}$)
7) Glu	0.500	0.574	0.408	0.318	0.532 ($P < 10^{-56}$)
8) Gly	0.727	0.771	0.614	0.633	0.642 ($P < 10^{-90}$)
9) His	0.022	0.026	−0.224	−0.300	−0.253 ($P < 10^{-11}$)
10) Ile	−0.403	−0.380	−0.136	−0.210	−0.233 ($P < 10^{-10}$)
11) Leu	0.237	0.091	−0.122	−0.050	−0.070 ($P < 0.1$)
12) Lys	−0.750	−0.654	−0.305	0.027	0.045 ($P < 0.3$)
13) Met	−0.620	−0.566	−0.337	−0.470	−0.484 ($P < 10^{-45}$)
14) Phe	0.421	0.417	0.351	0.527	0.495 ($P < 10^{-48}$)
15) Pro	0.382	0.244	0.091	0.392	0.467 ($P < 10^{-42}$)
16) Ser	−0.580	−0.612	−0.610	−0.600	−0.632 ($P < 10^{-86}$)
17) Thr	−0.730	−0.792	−0.794	−0.750	−0.765 ($P < 10^{-148}$)
18) Trp	0.722	0.723	0.573	0.653	0.661 ($P < 10^{-97}$)
19) Tyr	−0.250	−0.186	−0.035	−0.330	−0.362 ($P < 10^{-24}$)
20) Val	0.633	0.721	0.603	0.637	0.686 ($P < 10^{-107}$)

Note.—"Inclusive" gives the regression analysis including all amino acid sites of MMPs. "$S_{av} > d$" shows the analysis of amino acids with larger S_{av} than d. S_{av} is the moving average of local hydrophobic scores S around each amino acid site of MMPs (Materials and Methods). The helix domain was estimated by the primary structure analysis (ExPASy Proteomics Server; http://www.expasy.ch/; Gasteiger et al. 2005), using a standard model for the hydrophobic score (S) (Cowan and Whittaker 1990). "Helix cut" means that the estimated helix region with very low S_{av} values ($S_{av} < 0.1$) is excluded and the estimated nonhelix region with very high S_{av} values ($S_{av} > 0.7$) is included (supplementary fig. S2, Supplementary Material online). The numerical data show the correlation coefficient between each amino acid composition (AAC) and HYD. A main part of HYD variations was linked to three amino acids of glycine, valine, and tyrosine.

of table 1). As a result, a strong negative correlation between HYD and STC (fig. 1*B*) appeared in a hydrophobic domain of MMPs with $S_{av} > 0.1$. We here note that the separation method into the two groups provided mutually contrasting HYD and STC distributions characteristic of three terrestrial vertebrate groups comprising reptiles, birds, and placental mammals; STC values were small in fishes, intermediate in amphibians, and large in the terrestrial vertebrate groups (fig. 1*C*).

Introduction of mtRMR Having a Close Relationship with MLS as mt Trait

The Arrhenius-type equation (1) connected three variables (mtRMR, STC, and HYD) of mt functions to the ln(MLS) of an organism. First of all, we examined the first variable in equation (1), mtRMR = RMR/W^q. Here, if the number of cells is proportional to W and the mt density within cells is constant (independent of W), we can put $q = 1$. However, when we note that this density falls with increasing W (Porter and Brand 1995; Porter 2001), the q value must be less than 1. We determined the q value so as to maximize the correlation between X_1 = 1/mtRMR and Y = ln(MLS) and obtained $q = 0.84$ for placentals and $q = 0.87$ for birds (the q values were estimated by using a number of vertebrates (875 placentals and 983 birds in the AnAge data) without requiring the mt DNA data). These values improved the correlation coefficients between X_1 and Y, 0.514 for placentals and 0.663 for birds (table 2), because putting $q = 1$ gave the coefficients of 0.493 for placentals and 0.635 for birds. In this way, the mtRMR–MLS correlation is better than the RMR–MLS correlation (Rottenberg 2007). We assumed that the number of cells is proportional to W, and in fact, with the exception of the brain, organ size does indeed scale nearly isometrically with size (Peters 1986). In this way, mtRMR was identified as an important mt trait that can be related to MLS.

As is well known, body mass has been the best phenotypic predictor of MLS in placentals (Speakman 2005). Here, ln(MLS) gave a better correlation coefficient (0.493) with

Table 2
Correlation Coefficients for Pairs of the Variables X_1(1/mtRMR), X_2(1/STC), X_3(1/S_{av}) and Y{ln(MLS)} in Equation (1)

	$R_{1,Y}$	$R_{2,Y}$	$R_{3,Y}$	$R_{1,2}$	$R_{1,3}$	$R_{2,3}$
1) Placentals (80 species)	0.5141, $P < 10^{-5}$	−0.6893, $P < 10^{-11}$	0.4730, $P < 10^{-5}$	−0.1678, $P < 0.1$	−0.1772, $P < 0.4$	−0.7019, $P < 10^{-12}$
2) Cetaceans (18 species)	0.9163, $P < 10^{-7}$	0.7637, $P < 10^{-4}$	−0.6750, $P < 10^{-3}$	0.7350, $P < 10^{-3}$	−0.7861, $P < 10^{-4}$	−0.6982, $P < 10^{-3}$
3) Birds (32 species)	0.6628, $P < 10^{-4}$	−0.6259, $P < 10^{-4}$	0.4427, $P < 10^{-2}$	−0.4827, $P < 10^{-2}$	0.3345, $P < 10^{-1}$	−0.6325, $P < 10^{-3}$
4) Crocodilians (9 species)	—	0.7259, $P < 0.03$	−0.7148, $P < 0.03$	—	—	−0.6698, $P < 0.05$
5) Reptiles (15 species)	—	−0.7786, $P < 10^{-4}$	0.5537, $P < 0.03$	—	—	−0.7327, $P < 10^{-3}$
6) Amphibians (25 species)	—	0.5878, $P < 10^{-3}$	−0.4652, $P < 0.02$	—	—	−0.6444, $P < 10^{-4}$
7) Fishes (49 species)	—	0.4159, $P < 0.003$	−0.0689, $P < 0.65$	—	—	−0.3437, $P < 0.02$

Note.—Placentals exclude cetaceans, sirenians, rodents, and insectivores. Reptiles exclude crocodilians and turtles.

ln(W) than that (0.392) with W. This can be easily explained by the present approach in terms of 1/mtRMR: Using the excellent relationship between RMR and W, that is, ln(RMR) = α ln(W) + ln(β), we have approximately $X_1 = W^q$/RMR ≃ β$W^{q-\alpha}$. Here we derived $q - \alpha = 0.145$ for placentals (with α = 0.695 and β = 2.57). The quantity β$W^{q-\alpha}$ with such a small q value shows a similar behavior to ln(W) in large W values (>50 kg) (supplementary fig. S1, Supplementary Material online). Interestingly, the correlation coefficient (0.493) between ln(MLS) and β$W^{q-\alpha}$ in the case of $q = 1$ became equal to that between ln(MLS) and ln(W). We here note that mtRMR of placentals decreases with an increase in W, proportional to $W^{-0.14}$, whereas the mt maximum metabolic rate (mtMMR = MMR/W^q) rather increases with an increase in W; it is proportional to $W^{0.04}$ when we assume that MMR is proportional to $W^{0.88}$ (Bishop 1999).

Longevity Correlations with STC and HYD, Providing Sharp Contrast between Terrestrial Vertebrates and Marine Vertebrates (Cetaceans and Alligators)

Once mtRMR is identified as a variable of mt functions in the Arrhenius-type equation (1), other mt variables such as STC and HYD may be related to MLS. Table 2 lists the correlation coefficients ($R_{i,j}$) for all pairs of the variables $X_1 = 1$/mtRMR, $X_2 = 1$/STC, $X_3 = 1$/HYD, and Y = ln(MLS) in various vertebrate groups. Table 3 lists the correlation coefficients in the multiple regression analysis, showing that the coefficients give much better values than those in the single regression analysis and that MLS can be substantially described in terms of mtRMR and STC because of strong negative correlations between STC and HYD (table 2). In this regression analysis, we additionally included three proteins of ND1, ND3, and ND5 and determined the hydrophobic domains and proteins in each vertebrate group so as to maximize the correlation between X_2 and Y (supplementary table S1, Supplementary Material online) because these proteins were sometimes concerned to STC–MLS correlations, and the theoretical estimation of helix domain is not necessarily accurate (Materials and Methods). The regression analysis provided three distinct correlation patterns: (1) Terrestrial placentals (excluding cetaceans, sirenians, rodents, and insectivores), as well as birds and reptiles (excluding crocodilians), showed positive STC–MLS and negative HYD–MLS correlations; (2) secondarily aquatic vertebrates (those that returned to water from land such as cetaceans and crocodilians) and amphibians showed, on the contrary, negative STC–MLS and positive HYD–MLS correlations; and 3) primary aquatic vertebrates, that is, fishes, showed a weak STC–MLS correlation and no HYD–MLS correlation. The STC–MLS scatter diagrams of figure. 2*A* and *B* represent the mutually exclusive relationships in the two patterns of terrestrial placentals and cetaceans. The crocodilian lineage presents a similar behavior to the cetacean lineage, with low STC and long MLS for alligators and crocodiles and with high STC and short MLS for caimans (supplementary fig. S3, Supplementary Material online). We did not perform a regression analysis taking into account the tree structure (Felsenstein 1985; Harvey and Pagel 1991) because it is difficult to estimate reliable branch lengths in placental and bird trees, with problems such as simultaneous divergences, large evolutionary variations, and long-branch attractions (Kitazoe et al. 2007), although this analysis was useful for a local tree of the primate lineage (Kitazoe et al. 2008). However, the marked correlations between STC and MLS are so robust that they may be model independent of the analysis.

Relationship between Additional STC Increases and Very Large MLS Values in Primates

In placentals, STC showed a significant positive correlation with MLS (table 2 and fig. 2*A*). However, when STC is expressed in terms of 1/mtRMR, it represents markedly large values in hominoids and some other simians, which deviate strongly from the regression line of other placentals as outliers (the red circles in fig. 3*A*). A similar deviation was observed for MLS in terms of 1/mtRMR (the red circles in fig. 3*B*) and also in terms of ln(W) (supplementary fig. S4, Supplementary Material online). We here note that primates keep a middle position in the order of placentals as a function of 1/mtRMR (the red circles of fig. 3), whereas they occupy the highest side in the order of placentals as a function of STC (the red circles of fig. 2*A*).

Table 3

Multiple Correlation Coefficients for the Variables X_1(1/mtRMR), X_2(1/STC), X_3(1/S_{av}) and Y{ln(MLS)} in Equation (1)

	$R_{1+2,Y}$	$R_{1+3,Y}$	$R_{2+3,Y}$	$R_{1+2+3,Y}$
Placentals	0.7991, $P < 10^{-11}$	0.7488, $P < 10^{-8}$	0.6896, $P < 10^{-7}$	0.8106, $P < 10^{-15}$
Cetaceans	0.9259, $P < 10^{-4}$	0.9193, $P < 10^{-4}$	0.7889, $P < 10^{-3}$	0.9333, $P < 10^{-5}$
Birds	0.7492, $P < 10^{-3}$	0.7010, $P < 10^{-3}$	0.6288, $P < 10^{-3}$	0.7505, $P < 10^{-4}$
Crocodilians	—	—	0.7913, $P < 0.05$	—
Reptiles	—	—	0.7790, $P < 0.05$	—
Amphibians	—	—	0.5985, $P < 0.05$	—
Fishes	—	—	0.4233, $P < 0.05$	—

NOTE.—Placentals exclude cetaceans, sirenians, rodents, and insectivores. Reptiles exclude crocodilians and turtles. $R_{i+j,Y}$ denotes the correlation coefficient for the variables X_i, X_j, and Y{ln(MLS)}.

We have previously observed a large evolutionary change from hydrophobic amino acids to threonine in the primate lineage (Kitazoe et al. 2008). We adjusted the STC values of the primates so as to lie on the regression line for other placentals in figure 3*A* and also the MLS values of them so as to lie on the regression line for other placentals in figure 3*B*. As a result, we found that the location of the primates in placentals became consistent in both terms of 1/mtRMR and STC comparing figure 4 with figure 2*A*. This consistency strongly supports a close relationship between STC increase and MLS prolongation and provides the key to the biological meaning of STC.

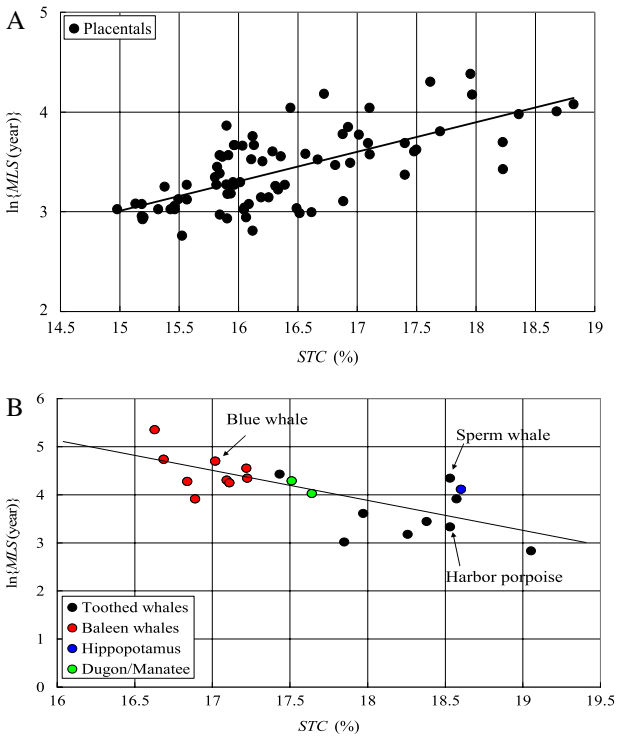

FIG. 2.—(*A*) Correlations between STC and ln(MLS) for placentals. (*B*): Correlations between STC and ln(MLS) for aquatic animals (cetaceans and sirenians). The placentals of (*A*) exclude cetaceans, sirenians, rodents, and insectivores. The regression line of (*B*) was given by only cetaceans. The hippopotamus is the sister group of cetaceans (supplementary fig. S7, Supplementary Material online). It is noteworthy that sirenians, with the same aquatic habitat, lie on the regression line, although they belong to Afrotheria, which is much far from Cetartiodactyla in the phylogenetic tree (Kitazoe et al. 2007).

Cysteine/Methionine–MLS Correlation of Rodents Induced by Oxidative Damages and Short Longevity in Early Mammalians

Rodents and insectivores were excluded from the STC–MLS analysis as they were outliers of the regression line for other

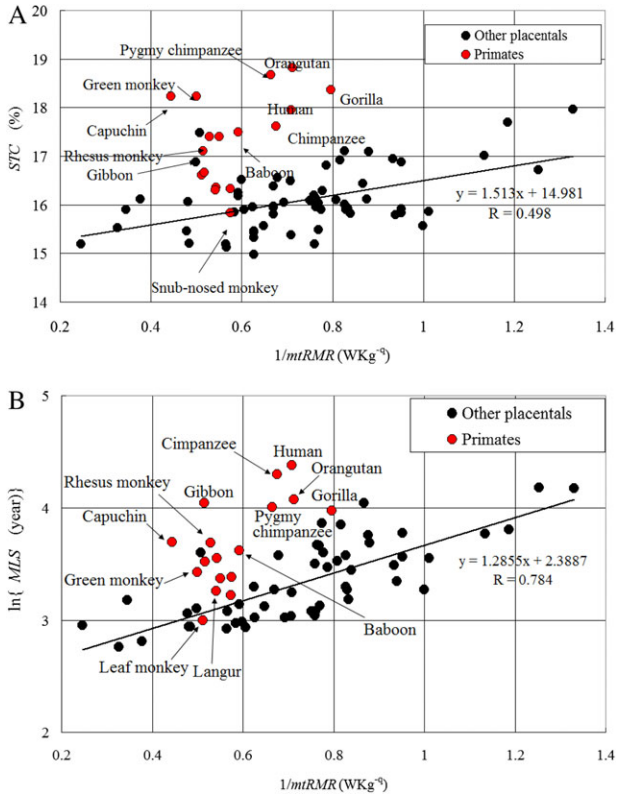

FIG. 3.—(*A*) Relationship between 1/mtRMR and STC in placentals. (*B*) Relationship between *1*/mtRMR and ln(MLS). The placentals of (*A*) exclude cetaceans, sirenians, rodents, and insectivores.

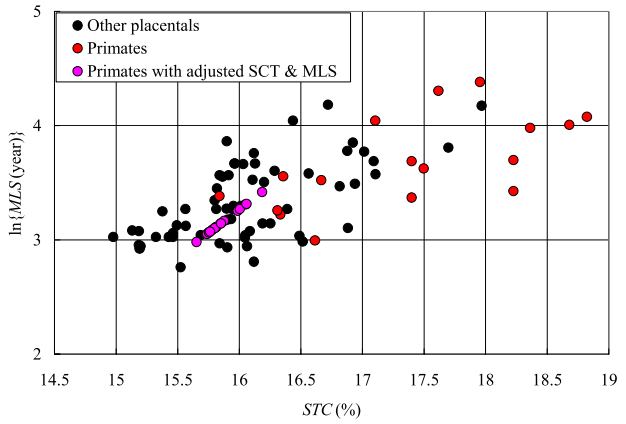

Fig. 4.—Relationship between STC and *Y* in placentals. *Y* stands for the theoretical value of ln(MLS) in equation (1). The circles are given by using the adjusted STC and HYD in equation (1).

placentals (excluding rodents, insectivores, and cetaceans) because there is no STC–MLS correlation with their very short MLS values (fig. 5) and very high mtRMR (fig. 6). Given their known high rates of free radical leak, we considered the possibility that the content of easily oxidized amino acids such as cysteine could be linked with their shorter life span, according to the proposal of Moosmann and Behl (2008). We examined amino acid residues, the compositions of which have negative correlations with MLS, and estimated the correlation coefficient *R* and *P* value between $X_4 = 1/\text{AAC}$ and $Y = \ln(\text{MLS})$ (here, AAC denotes an amino acid composition to be changed one after another by an iteration method). As a result, cysteine and methionine with sulfur atoms in their side chains showed significant correlations with *Y* in rodents (fig. 7*A*). Supplementary table S2 (Supplementary Material online) gives a criterion for selection of these two amino acids. Here, the selection of methionine may be consistent with a recent proposal that short-lived animals

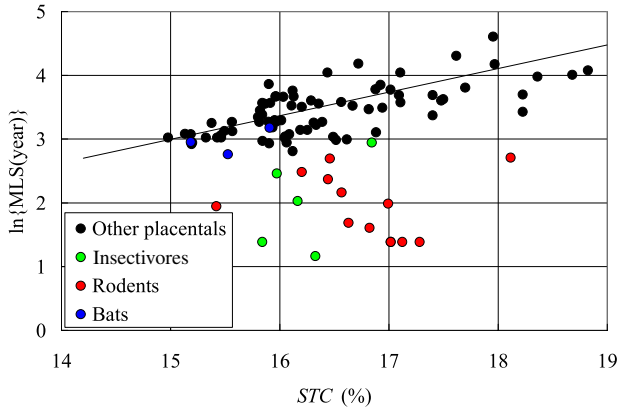

Fig. 5.—Relationship between *1*/mtRMR and ln(MLS) in rodents and insectivores. These animals became outliers of the regression line for other placentals (except for cetaceans and sirenians). This is the reason for why rodents and insectivores were excluded from STC–MLS analysis.

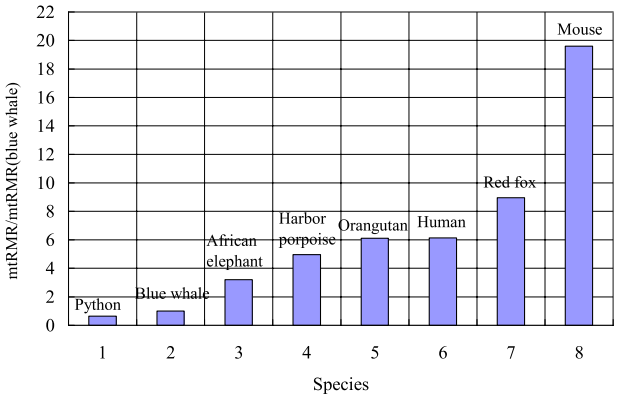

Fig. 6.—The mtRMR values in several animals, relative to that of blue whales.

subjected to higher oxidative stress selectively accumulate methionine in their mitochondrially encoded proteins, which supports the role of oxidative damage in aging (Aledo et al. 2011). In an individual analysis of respiratory chain complex subunits, complex I cysteine depletion is the almost exclusive carrier of the cysteine–life span correlation, whereas complex IV cysteine depletion is uniform in all aerobic animals, unrelated to longevity (Schindeldecker et al. 2011). The cysteine–MLS correlation in insectivores also seems significant (fig. 7*A*), but the number of sequences (five species) is insufficient for the statistical analysis. Here, insectivores include both Laurasiatherians and Afrotherians.

The absence of an STC–MLS correlation in rodents and insectivores suggested that mammals can be divided into two groups, the first with small MLS values and the second with large MLS values. We analyzed a number of MLS values of mammals using the AnAge database without the mtDNA data. The *t*-test for difference of means of ln(MLS) values between the two groups gave the best separation with $t = 33$ and $P < 10^{-150}$. Here, the first group included basal species such as Soricomorpha/Ernacemorpha (Laurasiatheria), Afrosoricida/Macroscelidea (Afrotheria), Rodentia/Lagomorpha (Supraprimates), Didelphimorphia (Ameridelphia), and Dasyuromorphia/Peramelemorpha (Australidelphia) (fig. 7*B*). Interestingly, only the placentals without STC–MLS correlation were automatically included in the first group. Because the lifestyles of the first group vertebrates are close to those of early mammals, it is possible that they retain mt functions reflecting an early stage of endothermic mammalian evolution.

Discussion

The present analysis uncovered a systematic correlation between HYD and STC throughout vertebrates. Terrestrial vertebrates showed decreases in HYD, increases in STC, and a positive correlation between STC, MLS, and increasing *W*. In stark contrast, marine vertebrates (cetaceans and alligators) showed an increase in HYD, a decrease in STC, and a negative correlation between STC and MLS. These

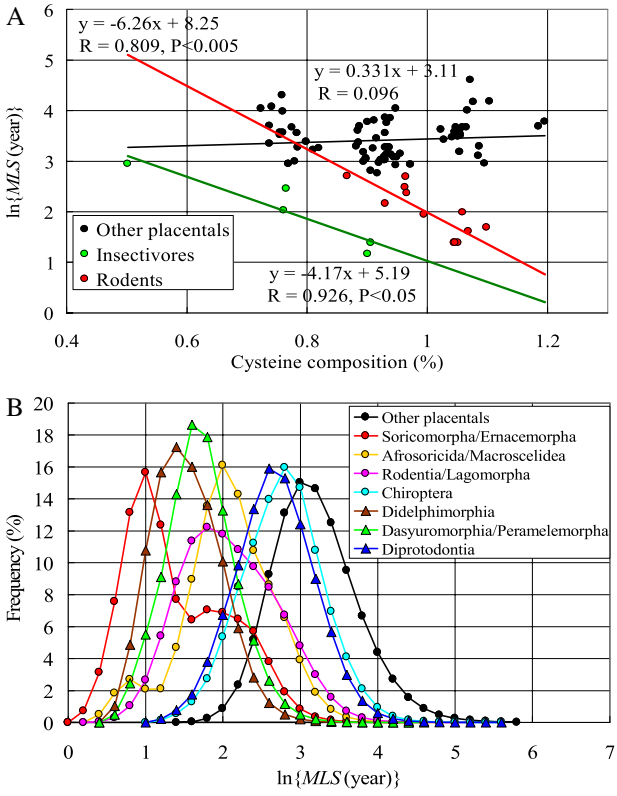

Fig. 7.—(*A*) Correlations between cysteine composition and ln(MLS) in rodents and insectivores. (*B*) Frequency distribution of ln(MLS) in eight mammalian groups with basal traits and the others (black circles). Rodents had significant correlations between cysteine composition and MLS for the sake of high rates of free radical leak and short MLS (supplementary table S2, Supplementary Material online). Bats (blue circles) with low STC values lie on the regression line (blue square denotes the average value and standard deviation of all 82 species included in the database (Allen 2003) but having no sequence data). The triangles of (*B*) denote marsupials. The distributions are largely separated into the two groups of the primitive species (Soricomorpha/Ernacemorpha, Afrosoricida/Macroscelidea, Rodentia/Lagomorpha, Didelphimorphia, and Dasyuromorphia/Peramelemorpha) and the others.

opposing evolutionary trajectories of the two animal groups provide a strong possibility that they are based on mt adaptation to the habitats and life strategies of vertebrates and not to nucleotide mutation pressure in the mt genomes. We discuss this possibility in more detail below, considering the stability and mobility of MMPs in the light of evolutionary demands.

Contrasting STC/HYD Behaviors Between Primates and Rodents in the Supraprimates

Although rodents and primates represented mutually quite different behaviors in STC and HYD, they are included in one of four major groups of placentals as the Supraprimates. Rodents do not show both the STC increase and the STC MLS correlation (fig. 5) but have high mtRMR (fig. 6) and high rates of free radical leak. Oxidative damage may be a critical factor in their life span. Indeed, they showed a strong negative correlation between cysteine composition and MLS in place of the STC–MLS correlation (fig. 7*A*), and their MLS values became very short in a sharp contrast to extremely long longevity in primates (hominoids), despite being within the same major group (figs. 3*B* and 5). One possible explanation is the central role of free radical signaling in selection for mitonuclear coadaptation, which in turn may enhance the fertility and adaptability of rodents, at the cost of shorter life span (Lane 2011a, 2011b).

Evolutionary Change of STC and HYD in Cetaceans, Describing Reversal over Time of Those in Terrestrial Vertebrates

The cetacean lineage represented a typical adaptive evolution, which contrasts with that of the terrestrial vertebrates, because STC and HYD values reverted toward those of fishes. We analyzed this evolutionary behavior in detail by further including sirenians and hippopotamus (fig. 2*B*). Cetaceans have a sister-group relationship with hippopotamus of artiodactyls (Nikaido et al. 1999) and form the lineage of Cetardiodactyla. They include toothed whales and baleen whales and the latter lineage being derived from the former lineage (supplementary fig. S5, Supplementary Material online) and evolved into animals with huge body masses. Toothed whales swim with fast maximum speeds, and water resistance increases in proportion to the square of velocity. Therefore, their STC values are high (fig. 2*B*), and mtRMR values are not low compared with their weights as seen in harbor porpoise (fig. 6). On the other hand, the baleen whales feed on plankton and krill by using giant filters and due to their huge body masses move underwater utilizing buoyancy to a large extent. This habitat allows for very low values of both mtRMR and aerobic capacity and also allows for a decrease in STC due to very low MMP mobility. As a result, MMP stabilization by an increase in HYD predominated and resulted in prolongation of the MLS of the baleen whales. Interestingly, sperm whales, which have a long MLS, deviated strongly from the regression line of cetaceans in figure 2*B*. This toothed whale also moves slowly with a huge body mass but nonetheless retains a high STC. One relevant feature of the sperm whale is that it dives deeply into the sea for food. Before diving, cold water enters the spermaceti organ. This solidifies the wax, and the increase in density generates a downward force that allows the whale to dive with less effort. The spermaceti is melted by a sudden rise in blood temperature, which increases its buoyancy, enabling easy surfacing (Clark 1970). The mt engine has to be quickly powered up to produce this rise of the blood temperature, that is, the sperm whale has a requirement for a rapid switch to high aerobic demand. This in turn requires a high STC for MMP stability.

A recent study reports that the basal swim speed of marine vertebrates increases with an increase in body mass (Watanabe et al. 2011). However, our interest is the difference between RMR and MMR. Indeed, the maximum swim speeds of dolphins are much higher than those in baleen whales. Unfortunately, both the RMR and the MLS data of marine vertebrates are poor at present. It would be interesting to investigate the adaptive evolution of these vertebrates in more detail. For example, the behavior of seals seems to be different from that of cetaceans (supplementary fig. S6*A*, Supplementary Material online) and rather similar to that of other placentals (supplementary fig. S6*B*, Supplementary Material online). They have a small variation of *W* values, and their divergence time (15 million years ago) is much later than that of cetaceans (50 million years ago). They belong to the carnivore lineage far from the cetartiodactyl lineage (including artiodactyls and cetaceans) and spend most of their time at sea, although they return to land or pack ice to breed and give birth and produce thick fat-rich milk that allows them to provide their pups with large amounts of energy in a short period. In fishes, STCs of tunas that swim fast with $W = 10–30$ (kg) and MLS = 10–20 (years) are located around the peak value of the distribution (fig. 1*C*), whereas those of eels with $W = 1–4$ (kg) and MLS = 20–80 (years) are located on the extreme right tail of the distribution.

Large STC/HYD Variations in Reptiles

The STC values of reptiles are divided into two regions, including relatively low values for lizards and very high values for some snakes (the second peak of reptiles in fig. 1*C*). Snakes have large STC values and small HYD values for their MMPs because of the negative correlation between these two values (table 2). Small HYD values enable MMP motility, which may be important for powering up the mt engine quickly. Interestingly, the true snakes such as boas, cobras, and pythons have among the highest STC values known. This may relate to their unusual eating habits. Such snakes often eat only every few months and have very low RMR values between meals to the point of dormancy. On eating a large meal (often 40% of body weight), their metabolic rates rise by 5- to 44-fold over several days, whereas their intestinal mass doubles and liver and kidney volumes increase by 50% (Secor and Diamond 1995; Secor 2003). Thus again, MMP mobility and stability depend not only on RMR but also on the kinetics: Abrupt changes in aerobic function apparently demand high MMP mobility, which is offset by interhelical STC stabilization. The reason of these speculations is discussed in the remaining paragraphs.

Why Do MMPs of Terrestrial Vertebrates Decrease HYD and Increase STC?

On the basis of the recent tertiary structural elucidation of complex I, the dynamic assembly of respirasome supercomplexes, and the speed of mt fusion and fission (Twig and Shirihai 2011), we assume that MMPs undergo large movements during their function and that their mobility and stability generally stand in a trade-off relationship (Hildebrand et al. 2008). The mtRMR and HYD in terrestrial vertebrates decrease with increasing *W*. The former decrease raises the stability of MMPs due to their lower mobility, whereas the latter decrease weakens their stability as they are embedded into the hydrophobic environment of lipid bilayer. By this compensation, they can retain their stability despite an increase in *W*. However, a severe problem takes place when the metabolic rate of an organism is accelerated from the RMR to the MMR around 5- to 10-fold greater than RMR (in fact, MMR of mammals scales with the 0.88 power of *W*, which is significantly different from 3/4 power scaling of RMR). It is determined by the energy needs of the cells active during "maximal work," and the aerobic capacity is higher in athletic than in nonathletic species (Bishop 1999; Porter 2001; Weibel et al. 2004; Weibel and Hoppeler 2005). In this way, the ratio mtMMR/mtRMR = MMR/RMR ($=W^{0.18}$) in mammals increases with an increase in *W*. The weakening of the hydrophobic effect permits greater mobility of MMPs, which in turn enables the elevation of mt functional activities. The cost is that MMPs become increasingly unstable.

Membrane proteins are stabilized by classical hydrogen bonds (Adamian and Liang 2002; Gimpelev et al. 2004), most of which are found in motifs involving medium polar residues such as serine or threonine. Indeed, it has been shown that such serine/threonine motifs can also drive the association of model transmembrane helices (Dawson et al. 2002). Thus, we propose that the STC increase in terrestrial vertebrates could compensate for the lack of the hydrophobic effect and provide the driving force for membrane protein folding (Eilers et al. 2000). In particular, we argue that the stabilization of transmembrane helices by hydrogen bonding could contribute to the dynamic assembly of respirasome supercomplexes at high rates of ATP synthesis, which in turn could speed electron flux via quantum tunneling within the solid-state respirasome model originally proposed by Chance and Williams (1955).

Relationship between MMP Stability and Longevity Derived From Arrhenius Plot Analysis

The Arrhenius plot analysis is commonly applied to predicting the stability of drugs (Lachman and DeLuca 1976; Ertel and Carstensen 1990; Carstensen 2000). The stability test is made under the stress condition of accelerated temperatures and therefore called temperature-accelerated stability study. The stability is given by the degradation rate of the plot. In analogy to this study, we transform equation (1) into its original form, $F(\text{mtMR}) = \exp(A_1/\text{MR} + A_2/\text{STC} + A_3/\text{HYD} + A_0) = F_0 \cdot \exp(A_1/\text{mtMR})$, and follow the *F* value as a function of mtMR, which goes from mtRMR to mtMMR. Here, the constants A_n ($n = 0–3$) are determined in advance by the regression analysis of each vertebrate group. The Arrhenius

plot describes the fall in stability of MMPs with rising mtMR values in an each animal. For example, the African elephant, with a very low mtRMR (fig. 6), shows a rapidly decreasing function of F with an increase in mtMR, whereas the red fox, with a high mtRMR, shows a slowly decreasing function of F with an increase in mtMR (supplementary fig. S7, Supplementary Material online). Because mtMMR is generally around 5- to 10-fold greater than mtRMR (Bishop 1999; Porter 2001), the F value in this region is almost saturated at its lowest level and insensitive to the precise value of mtMMR in each animal. The maximum value of the fall in stability is given by SF = F(mtRMR) − F(mtMMR), which stands for the degradation of MMP stability induced by accelerating the mt metabolic rate of an organism.

If this fall in stability is recovered by helix–helix interactions of hydrogen bonding, STC should provide positive correlations with SF because serine/threonine motifs are quite important for stabilizing the tertiary structure of MMPs. Such a correlation is demonstrated in placentals in which extensive STC increases and HYD decreases were observed in hominoids of the primate lineage (supplementary fig. S8, Supplementary Material online). We adjusted the STC and HYD values of primates so as to lie on the regression lines (blue lines) for many other placentals. We estimated the Y values of equation (1) by using these adjusted values and compared them with the original Y values as functions of STC (supplementary fig. S9, Supplementary Material online). As a result, the position of primates became very similar to that of figure 4 because the relationship between STC and Y in primates returned to that between STC and Y in other placentals. This result enables us to speculate that the MMP stabilization attained by additional STC increases in hominoids and some simians offset the fall in MMP stability at accelerated mt metabolic rates associated with a marked prolongation of longevity. A more rigorous estimation of MMP stability will need to be made in the future on the basis of a detailed tertiary structure analysis of MMPs, for example, with help of the molecular dynamics.

Long-Range Helix–Helix Interactions Taking Into Account Mobility of MMPs

Helix–helix (hydrogen bonding) interactions by serine/threonine motifs have normally a short range around 2Å and below 3Å. However, we note here that MMPs dynamically move during functions (Hildebrand et al. 2008) as one MMP complex (complex I) resembles a steam engine in which a piston drives a set of discontinuous helices (Efremov et al. 2010). As a result, even hydrogen-bonding pairs with larger distances (R) than 3Å can enter the short range when they oscillate with an amplitude (ΔR), which is enlarged with an increase in mt metabolic rates (functional activities). In addition, it is increasingly clear from blue-native gel electrophoresis (Dudkina et al. 2010) and flux-control analyses (Acín-Pérez et al. 2008; Genova et al. 2008; Lenaz and Genova 2009) that the random diffusion model of mt respiratory chain function is not supported at higher metabolic rates. Instead, dynamic respirasomes—comprising complexes I and III or I, III, and IV and possibly the ATP synthase (Acín-Pérez et al. 2008)—form stable supercomplexes during active oxidative phosphorylation. The dissociation of supercomplexes appears to depend on the electrical properties of the inner membrane, notably the membrane potential (Lenaz and Genova 2009), and we postulate that the dynamic assembly and disassembly of these respiratory supercomplexes could explain the high ST content of MMPs in animals with high aerobic capacity. The high ST content of MMPs may also stabilize respirasomes during mt fusion and fission, both highly dynamic processes associated with changes in electron flux and membrane potential, taking place in a matter of minutes (Twig and Shirihai 2011). We therefore postulate that the ability of serine and threonine residues to form both short-range and long-range hydrogen bonds assists in the formation of dynamic supercomplexes in the context of cristae remodeling and changes in respiratory flux.

We simulated how much the short-range force of a two-body potential can be effectively enlarged by the oscillation effect by applying a "spring" model in which a relative distance of hydrogen bond oscillates with the average amplitude ΔR around R. Obeying Hooke's law, we have mtMR = $K_0\,(\Delta R/R)^2$ with a constant K_0 (mtMR goes from mtRMR to mtMMR), and ΔR^2 becomes proportional to mtMR. The effective two-body potential and interaction range are given by $E(R) = (2\cdot\pi\cdot\Delta R^2)^{-1}\cdot\int\exp\{-(R - r)^2/(2\cdot\Delta R^2)\}\cdot H(r)\cdot dr$ and $R_{\mathrm{eff}} = \int R\cdot E(R)\cdot dR/\int E(R)\cdot dR$, respectively. Here, $H(r)$ denotes the original two-body potential of a short range. As a result, we confirmed that the effective interaction range R_{eff} can easily become two to three times as large as the original range (supplementary fig. S10, Supplementary Material online; the caption describes a detailed procedure to calculate R_{eff}). Occurrence of such a long-range potential markedly amplifies a probability of helix–helix interactions in the 3D configuration space associated with an increase in STC.

Possibility of Other Types of Adaptive Evolution

There is an inverse relationship between MLS and the proportion of $n - 3$ polyunsaturated fatty acids in lipids, which are sensitive to peroxidation (Pamplona et al. 2002; Hulbert et al. 2007). The behavior of fatty acid composition seems similar to that of the mtRMR because these two variables decrease with increases in W and MLS. It is interesting to include this fatty effect as an additional variable of mt composition in equation (1) for the multiple regression analysis when more data are available in the future. Other factors, such as the effect of proton leak on mt membrane surface area (Porter 2001), could also be examined by using equation (1).

It is noteworthy that the hydrophobicity of MMPs is subject to reversible selection in terrestrial vertebrate groups. One of the main hypotheses for the retention of mtDNA at all relates to the physical intractability of hydrophobic MMPs. On the basis of our study, MMP hydrophobicity is indeed tractable to selection, so an inability to alter the properties of MMPs does not seem to be sufficient reason to retain mtDNA. Other factors, such as redox regulation—the requirement for locally calibrated changes in expression of mt genes in response to changes in supply and demand as reflected in redox state and membrane potential—presumably play an important role. The findings presented here are consistent with the colocation for redox regulation hypothesis (Allen 2003).

Concluding Remarks

In examining how mitochondria have been adapted to the habitats and life strategies of vertebrates, we analyzed the behavior of HYD and STC in various vertebrate groups. As a result, we speculate that low HYD and high STC are linked to increases in MMP mobility and stability in terrestrial vertebrates, and these features are then related to energetic requirements and longevity of them. These speculations were derived almost entirely within the framework of Arrhenius equation.

Supplementary Material

Supplementary tables S1 and S2 and figures S1–S9 are available at *Genome Biology and Evolution* online (http://www.gbe.oxfordjournals.org/).

Acknowledgments

Y.K. thanks Kozo Utsumi and Junichiro Futami (Okayama University) and Keiko Udaka (Kochi Medical School) for constructive discussions and insights. This work was supported by grants from Japanese Society for the Promotion of Science (22570099 to M.H.); Grants-in-Aid for Scientific Research from the Ministry of Education, Culture, Sports, Science, and Technology of Japan (A-22240072 and B-21390459 to M.T.); grant 20B-13 from the program Research Grants for Nervous and Mental Disorders of the Ministry of Health, Labour, and Welfare (to M.T.); and grants for scientific research from the Takeda Science Foundation (to M.T.). N.L. is grateful to the UCL Provost's Venture Research Fellowship for Support.

Literature Cited

Accelerated life testing analysis theory & principles [Internet]. [cited 2011 Sept 1]. Available from: http://www.weibull.com/acceltestwebcontents.htm

Acín-Pérez R, Fernández-Silva P, Peleato ML, Pérez-Martos A, Enriquez JA. 2008. Respiratory active mitochondrial supercomplexes. Mol Cell. 32:529–539.

Adamian L, Liang J. 2002. Interhelical hydrogen bonds and spatial motifs in membrane proteins: polar clamps and serine zippers. Proteins 47:209–218.

Aledo JC, Li Y, de Magalhães JP, Ruíz-Camacho M, Pérez-Claros JA. 2011. Mitochondrially encoded methionine is inversely related to longevity in mammals. Aging Cell 10(2):198–207.

Allen JF. 2003. The function of genomes in bioenergetic organelles. Phil Trans R Soc Lond. B358:19–37.

Bishop CM. 1999. The maximum oxygen consumption and aerobic scope of birds and mammals: getting to the heart of the matter. Proc R Soc Lond B Biol Sci. 266:2275–2281.

Bromham L, Rambaut A, Harvey PH. 1996. Determinants of rate variation in mammalian DNA sequence evolution. J Mol Evol. 43:610–621.

Carstensen JT. 2000. Solution kinetics. In: Carstensen JT, Rhodes CT, editors. Drug stability: principles and practices (3rd ed.). New York: Marcel Dekker. p. 19–55.

Chance B, Williams GR. 1955. A method for the localization of sites for oxidative phosphorylation. Nature 176:250–254.

Clark M. 1970. Function of spermaceti organ of the sperm whale. Nature 228:873–874.

Cowan R, Whittaker RG. 1990. Hydrophobicity indices for amino acid residues as determined by high-performance liquid chromatography. Pept Res. 3:75–80.

Dawson JP, Weinger JS, Engelman DM. 2002. Motifs of serine and threonine can drive association of transmembrane helices. J Mol Biol. 316:799–805.

de Magalhaes JP, Costa J. 2009. A database of vertebrate longevity records and their relation to other life-history traits. J Evolution Biol. 22:1770–1774. Available from: http://genomics.senescence.info/species/.

Dudkina NV, Kouril R, Peters K, Braun HP, Boekema EJ. 2010. Structure and function of mitochondrial supercomplexes. Biochim Biophys Acta Bioenerg. 1797:664–670.

Efremov RG, Baradaran R, Sazanov LA. 2010. The architecture of respiratory complex. Nature 466:441–445.

Eilers M, Shekar SC, Shieh T, Smith SO, Fleming PJ. 2000. Internal packing of helical membrane proteins. Proc Natl Acad Sci USA. 97:5796–5801.

Ertel KD, Carstensen JT. 1990. Examination of a modified Arrhenius relationship for pharmaceutical stability prediction. Int J Pharm. 61:9–14.

Felsenstein J. 1985. Phylogenies and the comparative method. Am Nat. 125:1–15.

Galtier N, Jobson RW, Nabholz B, Glemin S, Blier PU. 2009. Mitochondrial whims: metabolic rate, longevity and the rate of molecular evolution. Biol Lett. 5:413–416.

Garey JR, Judge DS. 2002. Longevity records: life spans of mammals, birds, amphibians, reptiles, and fish. Odense (Denmark): Odense University Press. Available from: http://www.demogr.mpg.de/longevityrecords/.

Gasteiger E, Hoogland C, Gattiker A, Duvaud S, Wilkins MR, Appel RD, Bairoch A. 2005. Protein identification and analysis tools on the ExPASy server. In Walker JM, editor. The proteomics protocols handbook. Totowa (NJ): Humana Press. p. 571–607. Available from: http://www.expasy.ch/.

Genova ML, et al. 2008. Is supercomplex organization of the respiratory chain required for optimal electron transfer activity? Biochim Biophys Acta Bioenerg. 1777:740–746.

Gibson A, Gowri-Shankar V, Higgs PG, Rattray M. 2005. A comprehensive analysis of mammalian mitochondrial genome base composition and improved phylogenetic methods. Mol Biol Evol. 22:251–264.

Gillooly JF, McCoy MW, Allen AP. 2007. Effects of metabolic rate on protein evolution. Biol Lett. 3:655–659.
Gimpelev M, Forrest LR, Murray D, Honig B. 2004. Helical packing patterns in membrane and soluble proteins. Biophys J. 87:4075–4086.
Goldberg A, et al. 2003. Adaptive evolution of cytochrome c oxidase subunit VIII in anthropoid primates. Proc Natl Acad Sci. USA. 100:5873–5878.
Grossman LI, Schmidt TR, Wildman DE, Goodman M. 2001. Molecular evolution of aerobic energy metabolism in primates. Mol Phylogenet Evol. 18:26–36.
Harvey PH, Pagel MD. 1991. The comparative method in evolutionary biology. Oxford: Oxford University Press.
Hildebrand PW, et al. 2008. Hydrogen-bonding and packing features of membrane proteins: functional implications. Biophys J. 94:1945–1953.
Hulbert AJ, Pamplona R, Buffenstein R, Buttemer WA. 2007. Life and death: metabolic rate, membrane composition, and life span of animals. Physiol Rev. 87:1175–1213.
Jobson RW, Dehne-Garcia A, Galtier N. 2010. Apparent longevity-related adaptation of mitochondrial amino acid content is due to nucleotide compositional shifts. Mitochondrion 10:540–547.
Kitazoe Y, et al. 2007. Robust time estimation reconciles views of the antiquity of placental mammals. PLoS One. 2:e384.
Kitazoe Y, et al. 2008. Adaptive threonine increase in transmembrane regions of mitochondrial proteins in higher primates. PLoS One. 3:e3343.
Lachman L, DeLuca P. 1976. Kinetic principles and stability testing. The theory and practice of industrial pharmacy (2nd ed.). Philadelphia (PA): Lea and Febiger. p. 32–69.
Lane N. 2006. Power, sex, suicide: mitochondria and the meaning of life. New York: Oxford Univ Press.
Lane N. Forthcoming. 2011a. The evolutionary tradeoffs of breathing. Science.
Lane N. Forthcoming. 2011b. Mitonuclear match: optimizing fitness and fertility over generations drives ageing within generations. BioEssays.
Lehmann G, Segal E, Muradian KK, Fraifeld VE. 2008. Do mitochondrial DNA and metabolic rate complement each other in determination of the mammalian maximum longevity? Rejuvenation Res. 11:409–417.
Lenaz G, Genova ML. 2009. Structural and functional organization of the mitochondrial respiratory chain: a dynamic super-assembly. Int J Biochem Cell Biol. 41:1750–1772.
Min XJ, Hickey DA. 2008. An evolutionary footprint of age-related natural selection in mitochondrial DNA. J Mol Evol. 67:412–417.
Moosmann B, Behl C. 2008. Mitochondrially encoded cysteine predicts animal lifespan. Aging Cell 7:32–46.
Moser CC, Page CC, Dutton PL. 2006. Darwin at the molecular scale: selection and variance in electron tunnelling proteins including cytochrome c oxidase. Phil Trans Roy Soc B. 361:1295–1305.
Nabholz B, Glemin S, Galtier N. 2009. The erratic mitochondrial clock: variations of mutation rate, not population size, affect mtDNA diversity across birds and mammals. BMC Evol Biol. 9:54.
NCBI Genome Database [Internet]. Bethesda (MD): The National Center for Biotechnology Information [cited 2011 Jun 25]. Available from: http://www.ncbi.nlm.nih.gov/genomes/.
Nikaido M, Rooney AP, Okada N. 1999. Phylogenetic relationships among cetartiodactyls based on insertions of short and long interpersed elements: hippopotamuses are the closest extant relatives of whales. Proc Natl Acad Sci USA. 96:10261–10266.
Pamplona R, Barja G. 2007. Highly resistant macromolecular components and low rate of generation of endogenous damage: two key traits of longevity. Ageing Res Rev. 6:189–210.
Pamplona R, Barja G, Portero-Otín M. 2002. Membrane fatty acid unsaturation, protection against oxidative stress, and maximum life span: a homeoviscous-longevity adaptation? Ann N Y Acad Sci. 959:475–990.
Peters RH. 1986. The ecological implications of body size. Cambridge: Cambridge University Press. p. 329. ISBN 0-521-2886-x.
Pontzera H, Raichlenb DA, Shumakerc RW, Ocobocka C, Wiche SA. 2010. Metabolic adaptation for low energy throughput in orang-utans. Proc Natl Acad Sci USA. 107:14048–14052.
Porter RK. 2001. Allometry of mammalian cellular oxygen consumption. Cell Mol Life. 58:815–822.
Porter RK, Brand MD. 1995. Causes of the difference in respiration rates from mammals of different body mass. Am J Physiol. 269:R1213–R1224.
Reyes A, Gissi C, Pesole G, Saccone C. 1998. Asymmetrical directional mutation pressure in the mitochondrial genome of mammals. Mol Biol Evol. 15:957–966.
Rottenberg H. 2007. Coevolution of exceptional longevity, exceptionally high metabolic rates, and mitochondrial DNA-coded proteins in mammals. Exp Gerontol. 42(4):364–373.
Schindeldecker M, Stark M, Behl C, Moosmann B. 2011. Differential cysteine depletion in respiratory chain complexes enables the distinction of longevity from aerobicity. Mech Ageing Dev. 132(4):171–179.
Schmitz J, Ohme M, Zischler H. 2002. The complete mitochondrial sequence of Tarsius bancanus: evidence for an extensive nucleotide compositional plasticity of primate mitochondrial DNA. Mol Biol Evol. 19:544–553.
Secor SM. 2003. Gastric function and its contribution to the post-prandial metabolic response of the Burmese python *Python molurus*. J Exp Biol. 206:1621–1630.
Secor SM, Diamond J. 1995. Adaptive responses to feeding in Burmese pythons: pay before pumping. J Exp Biol. 198:1313–1325.
Speakman JR. 2005. Body size, energy metabolism and lifespan. J Exp.Biol. 208:717–1730.
Spradling T, Hafner M, Demastes J. 2001. Differences in rate of cytochrome-b evolution among species of rodents. J Mammal. 82:65–80.
Twig G, Shirihai OS. 2011. The interplay between mitochondrial dynamics and mitophagy. Antioxid Redox Signal. 14:1939–1951.
Watanabe Y, et al. 2011. Scaling of swim speed in breath-hold divers. J Anim Ecol. 80:57–68.
Weibel ER, Bacigalupe LD, Schmitt B, Hoppeler H. 2004. Allometric scaling of maximal metabolic rate in mammals: muscle aerobic capacity as determinant factor. Respir Physiol Neurobiol. 140(2):115–132.
Weibel ER, Hoppeler H. 2005. Exercise-induced maximal metabolic rate scales with muscle aerobic capacity. J Exp Biol. 208(Pt 9):1635–1644.
Welch JJ, Bininda-Emonds OR, Bromham L. 2008. Correlates of substitution rate variation in mammalian protein-coding sequences. BMC Evol Biol. 8:53.

Associate editor: Bill Martin